Charge Trajectory Optimization of Plug-in Hybrid Electric Vehicles for Energy Cost Reduction and Battery Health Enhancement

Saeid Bashash, Scott J. Moura, and Hosam K. Fathy*

***Abstract*— This paper examines the problem of optimizing the *charge trajectory* of a plug-in hybrid electric vehicle (PHEV), defined as the timing and rate with which the PHEV obtains electricity from the power grid. Two objectives are considered in this optimization. First, we minimize the total cost of fuel and electricity consumed by the PHEV over a 24-hour naturalistic drive cycle. We predict this cost using a previously-developed stochastic optimal PHEV power management strategy. Second, we also minimize total battery health degradation over the course of the 24-hour cycle. This degradation is predicted using an electrochemistry-based model of anode-side resistive film formation in Li-ion batteries. The paper shows that these two objectives are conflicting, and trades them off using a non-dominated sort genetic algorithm, NSGA-II. As a result, a Pareto front of optimal PHEV charge trajectories is obtained. The effects of electricity price and trip schedule on the Pareto front are analyzed and discussed.**

I. Introduction

This paper examines *plug-in hybrid electric vehicles (PHEVs)*, defined as vehicles that can use both fuel and battery electricity for propulsion, and can obtain the latter either through onboard generation or by plugging into the grid. The paper's overarching goal is to optimize the *charge trajectory* of such PHEVs, defined as the timing and the rate which they obtain electric energy from the grid. We perform this optimization with two objectives in mind, namely, *(i)* minimizing the overall cost of daily PHEV energy consumption and *(ii)* minimizing the concurrent damage to PHEV batteries. Such optimization is an important step towards achieving the potential economic and environmental benefits of PHEVs envisioned by the scientific community [1-5]. Moreover, the optimal charge trajectories can be used to build a spatiotemporal predictive model for the PHEV load on the grid, assuming that consumers will adopt these optimal charging strategies.

*Address all correspondence to this author, hfathy@umich.edu. Authors are with the Control Optimization Laboratory, Department of Mechanical Engineering, the University of Michigan, Ann Arbor, MI 48109.

The research presented in this paper was funded by a Michigan Public Service Commission (MPSC) grant to a research partnership including The University of Michigan, DTE Energy, and other partners. The authors would like to acknowledge this support from MPSC. Any opinions, findings, and conclusions or recommendations expressed in this material are those of the authors and do not necessarily reflect the views of the funding agencies or research partners. Authors would like to also thank Prof. Zoran Flipi, Dr. Tae-Kyung Lee, Dr. Karim Hamza and Joel Forman for their valuable help and support.

The literature has examined PHEV charge trajectories from a number of different perspectives. The most common conjecture in this respect is the overnight charging scenario, which assumes PHEVs will start charging late at night, e.g., 10 p.m. or midnight [4-6]. Evening charging is another scenario which has also been examined [5]. More sophisticated trip- and price-dependent strategies such as "immediate end of travel", "optimized to off-peak", and "opportunity charging" have also been assumed and used for the prediction of PHEV load [6]. This paper optimizes PHEV charging in a way that takes into account, for the first time, the combined effects of total energy cost, battery health, electricity pricing, and the PHEV's driving pattern. The charge trajectories obtained through this optimization are substantially different from those optimized for energy cost or battery health alone.

One of the necessary and most expensive elements of PHEVs is their high-capacity battery storage system which tends to degrade with time and cycling [7-9]. This paper focuses specifically on PHEVs that use Lithium-ion batteries for such storage. The literature on the modeling of Li-ion batteries is essentially divided into two main categories: (*i*) Empirical models that are built upon the experimental observations of battery input/output behavior, such as equivalent circuit models [10, 11], and (*ii*) high-fidelity models that are derived from the first principles of battery electrochemistry [12, 13]. The modeling of capacity fade and life degradation has been more extensively pursued under the second category. This paper adopts a first-principles electrochemistry-based battery model developed by Doyle *et al.* [12] and Fuller *et al.* [13], and later expanded by Ramadass *et al.* [14] through the addition of a capacity fade component. In this model, the battery degradation mechanism is governed by a side reaction within the negative electrode (anode), resulting in the formation of an irreversible solid electrolyte interface (SEI) film on the electrode, and the loss of cyclable lithium ions. Although there are several other degradation mechanisms for the Li-ion batteries, such as overheating, overcharging, deep discharging, etc. [15], in this paper we only consider the SEI film formation as the primary cause of battery degradation. The approach we adopt in this effort is generalizable to other mechanisms as well.

To the best of the authors' knowledge, there are currently no published articles in the PHEV literature that optimize the charge trajectory of PHEVs for both energy cost and battery health. Thus, this paper is the first to analyze this problem. Since we deal with optimizing two objectives which are

conflicting (as will be explained in the paper), we use a multiobjective optimization algorithm, namely, the non-dominated sorting genetic algorithm II (NSGA-II) developed by Deb *et al.* [16]. Our goal is to obtain an optimal Pareto front that trades off the two objectives. To quantify the daily energy cost, we use a mid-size sedan PHEV model with a previously-developed optimal on-road power management strategy [17, 18], and a naturalistic 24-hour drive cycle with two (morning and afternoon) half trips. Moreover, the measure of battery degradation is obtained through a reduced order representation of the electrochemistry-based battery model discussed above. To account for the variation of the electricity price, we use the pricing policy of DTE Energy Company for electric vehicles in the State of Michigan [19]. Putting all the described elements together, we finally optimize the PHEV charge trajectory, and study various solutions from the obtained Pareto front.

The reminder of the paper is organized as follows: Section II provides a brief review of the PHEV model with optimal on-road power management strategy followed by a simulation study. In Section III, we review the Li-ion battery degradation model. Section IV formulates the charge trajectory optimization problem. In Section V, we review the NSGA-II for multiobjective optimization. In Section VI, we optimize the PHEV charge trajectories using NSGA-II, and provide extensive discussions. Finally, Section VII summarizes the paper's main conclusions.

II. PHEV Model and Optimal Power Management

The two objectives optimized in this paper, namely, energy cost and battery health, depend not only on PHEV charging, but also on how the given PHEV operates on the road. Therefore, modeling PHEV on-road power management is an important prerequisite to charge trajectory optimization. On-road power management can be optimized using a number of different methods, including deterministic dynamic programming (DDP), when the drive cycle is known [20, 21], and stochastic dynamic programming (SDP), when a statistical drive cycle description is available [17, 18]. This paper adopts a PHEV model used by the authors in a previous study [17] as well as the on-road power management algorithm optimized for that PHEV using SDP. We describe both briefly below.

A. PHEV Model

The PHEV model is based on a power-split mid-size sedan, similar in configuration, dynamics, and design to the 2002 Toyota Prius, but with an 8 kWh Li-ion battery pack. The supervisory power management algorithm, which determines the optimal split of engine and battery power, is developed using SDP. We summarize the PHEV model and associated optimal supervisory control strategy here for comprehensiveness, but readers are encouraged to read [17] for complete details.

Figure 1 presents a conceptual map of the key interactions between the PHEV examined in this paper, the drive cycle, and the supervisory power management algorithm. The supervisory power management algorithm attempts to meet drive cycle power demand by adjusting three control inputs: engine torque, electric motor/generator 1 (M/G1) torque, and M/G2 torque. These inputs are determined by a nonlinear static feedback law, which depends functionally on engine speed, vehicle velocity, battery SOC, and power demand.

The vehicle model consists of five components shown schematically in Figure 1: the engine, motor/generators, planetary gear set, longitudinal vehicle dynamics, and battery pack. The engine and motor/generator models are steady-state maps that respectively output fuel consumption rate and power efficiency as functions of speed and torque. The drive cycle is modeled as a first order Markov process. Models for the remaining components can be grouped in terms of the inertial dynamics, road loads, and battery SOC dynamics. The inertial dynamics form state equations for the speeds of the engine, M/G1, and M/G2 (directly proportional to vehicle velocity). These three speeds must satisfy a kinematic constraint created by the planetary gear set. The road loads represent forces acting against the PHEV's inertia, including rolling resistance, viscous air drag, and wheel/axle bearing friction. For the purposes of control optimization, the battery pack is idealized by an open circuit voltage in series with an internal resistance. The battery pack SOC dynamics are determined by integrating battery pack current.

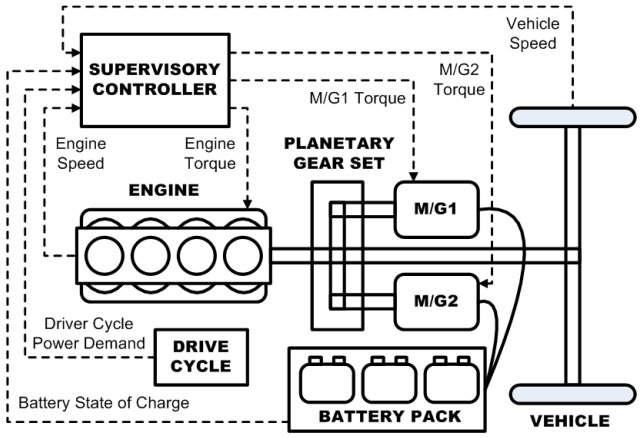

Fig. 1. PHEV model components, supervisory controller, and signal flow. Note that the signal flow forms a state feedback control architecture.

B. Simulations of Optimal Power Management in PHEVs

Figure 2 depicts a sample suburban naturalistic daily drive cycle with two separate trips. Using the model and the optimal power management strategy developed in [17] and explained above, we examine the battery discharge behavior, and fuel and electricity consumption costs, as the vehicle follows the given drive cycle (only the first segment of the drive cycle is considered for the simulations of this section). The electricity and the fuel prices are set to 0.08 USD/kWh (representative price for Midwest in the year 2008) and 3.44 USD/gallon (representative value for the year 2008), respectively.

Figure 3 depicts the simulation results for three different initial battery charge levels. Comparing the energy cost trajectories in Figure 3 implies that higher initial battery SOC results in higher electricity cost, but lower fuel and total energy cost at the end of the trip. This trend is due the use of a less costly energy source (i.e., electricity) for a longer portion of the trip, when the battery SOC is higher. Therefore, we can conclude: *The higher the initial battery SOC for a given trip, the less the total energy cost at the end of that trip, assuming that all the stored electricity is consumed.*

Now that we have shown the effects of battery charge on vehicle operating cost, we review a high-fidelity Li-ion battery model in the next section to demonstrate the effects of battery charge on its life degradation characteristics.

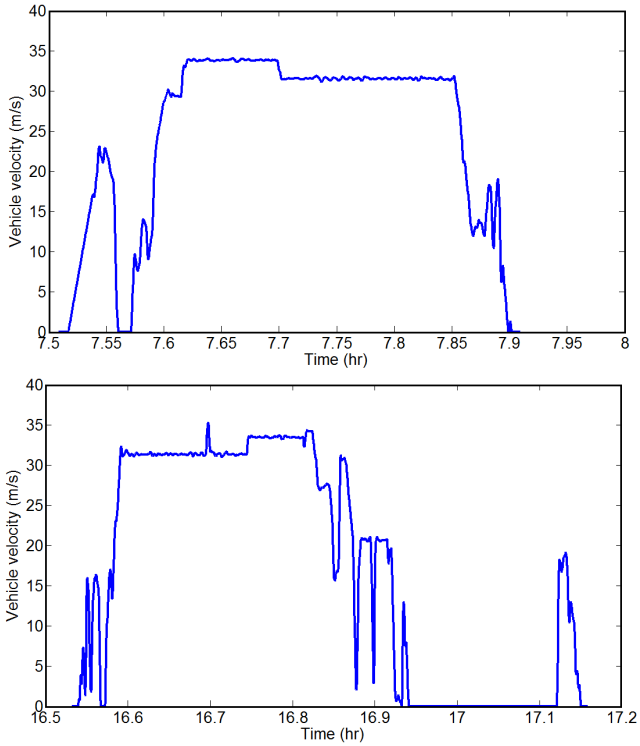

Fig. 2. A sample suburban naturalistic daily drive cycle with two trips.

III. High-Fidelity Li-ion Battery Model

The performance and long-term viability of PHEVs are highly dependent on their electrochemical batteries. Irreversible health degradation is a negative factor in these components that must be well understood prior to optimizing the charge trajectory. Efficient and accurate simulation of battery is a necessity, particularly in Vehicle-to-Grid applications.

The simulations in this paper are based a pseudo-2D electrochemical model that includes degradation effects [12-14], where the main degradation cause is an anodic side reaction. As a result of this reaction, a resistive film builds up in the anode which increases the internal resistance of battery and leads to capacity loss. This appears to be the model of lowest complexity that can both predict health degradation and work on a very wide range of cycles (due to its 1st principles nature). Simpler models have been used to monitor battery SOC and State-of-Health (SOH) [22-25]. However, these models have been developed to only observe the battery degradation effect, not to predict it. Hence, we cannot use them for battery health simulation and optimization.

The following section briefly reviews the battery model used in this paper for PHEV charge trajectory optimization.

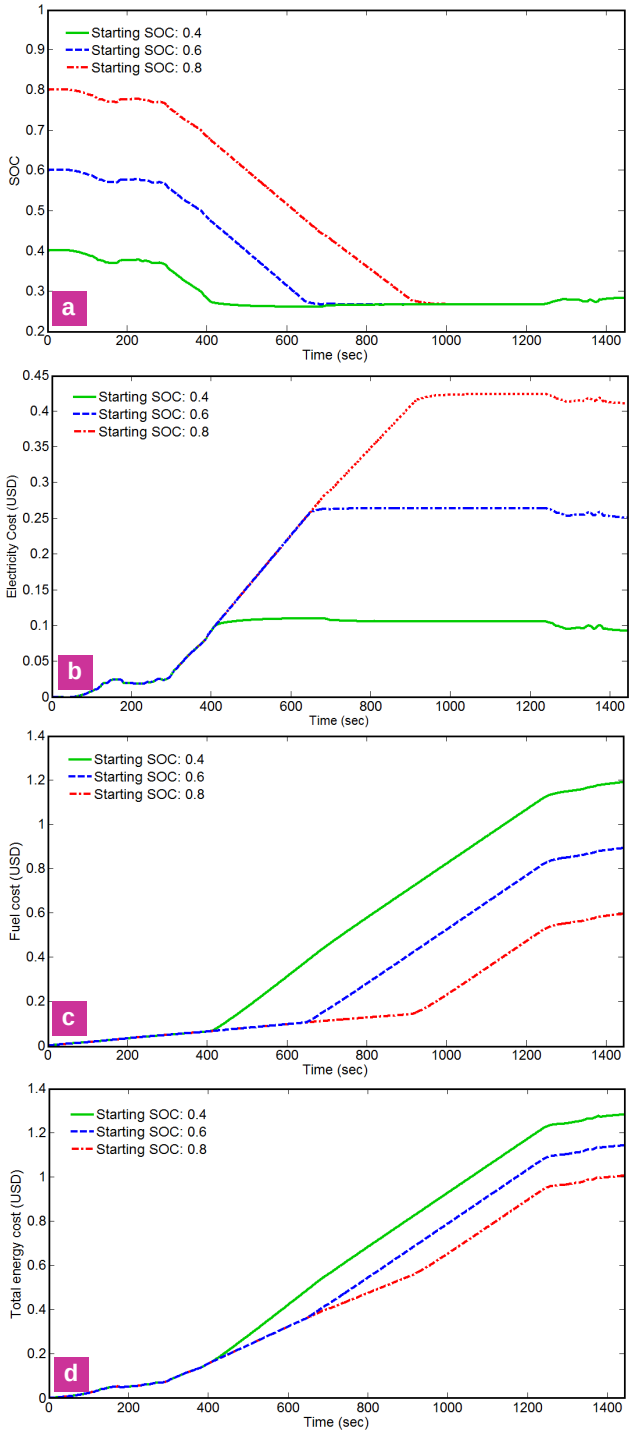

Fig. 3. Simulations of optimal PHEV power management and energy cost trajectories for different starting SOCs: (a) SOC plots, (b) electricity costs, (c) fuel costs, and (d) total energy costs.

A. Battery Model Review

Li-ion batteries store electric energy by shuffling lithium ions between low and high potential energy states via a set of electrochemical processes. Lithium ions have the lowest energy when they are in the cathode and the highest energy when they are in the anode. During charging, external current forces lithium ions to move from the cathode to the anode. During discharge, ions naturally move from the anode to the cathode, creating a useful current. Lithium ions movement is governed by two diffusion processes, and two electrochemical reactions driven by overpotentials. These reactions allow the lithium ions to transfer between solid and solution phases via intercalation currents.

This paper adopts the Li-ion battery model originally developed by Doyle, Fuller and Newman [12, 13] with a degradation model added later by Ramadass *et al.* [14]. Based on this model, the governing equations of solid phase and solution phase potentials (denoted by ϕ_1 and ϕ_2, respectively) are given by Ohm's law as follows*:

$$\nabla \cdot \left(\sigma_j^{eff} \nabla \phi_{1,j} \right) - J = 0, \; j = n, p \tag{1}$$

$$\nabla \cdot \left(\kappa^{eff} \nabla \phi_2 \right) + \nabla \cdot \left(\kappa_D \nabla \ln \left(c_2 \right) \right) + J = 0 \tag{2}$$

where σ_j^{eff} is the effective conductivity of electrode j (where n stands for the negative, and p for the positive electrode), κ^{eff} and κ_D respectively represent the concentration-dependent effective and diffusional conductivities of the solution phase, and $J = J_1 + J_{sd}$ is the total intercalation current density calculated from the main reaction given by:

$$J_1 = a_j i_{0,j} \left[\exp\left(\frac{\alpha_{a,j} F}{RT} \eta_j \right) - \exp\left(-\frac{\alpha_{c,j} F}{RT} \eta_j \right) \right], \; j = n, p \tag{3}$$

where

$$i_{0,j} = k_j \left(c_{1,j}^{\max} - c_{1,j}^{S} \right)^{\alpha_{a,j}} \left(c_{1,j}^{S} \right)^{\alpha_{c,j}} \left(c_2 \right)^{\alpha_{a,j}}, \; j = n, p \tag{4}$$

and a side reaction governed by:

$$J_{sd} = -i_{0,sd} a_n \exp\left(-\frac{\alpha_{c,n} F}{RT} \eta_{sd} \right) \tag{5}$$

where a and k are the specific area of the porous electrode and the rate constant of electrochemical reaction, respectively; α_a and α_c are the anodic and cathodic transfer coefficients of electrochemical reaction; F, R, and T respectively denote the Faraday's constant, universal gas constant and the temperature; c_1 and $c_1^{\max}$ represent the lithium concentration in the solid phase, and its maximum limit; i_0 and $i_{0,sd}$ are the exchange current densities for the main and the side reactions, respectively , and η and η_{sd} are the corresponding overpotentials, given by:

$$\eta_j = \phi_1 - \phi_2 - U_{ref,j} - \frac{J}{a_n} R_{film}, \; j = n, p \tag{6}$$

$$\eta_{sd} = \phi_1 - \phi_2 - U_{ref,sd} - \frac{J}{a_n} R_{film} \tag{7}$$

* *List of all parameter values and the boundary conditions for the partial differential equations, i.e. (1), (2), (8) and (9), can be found in [26].*

where $U_{ref,j}$ is the SOC-dependent equilibrium potential of the main reaction, R_{film} is the side film resistance in anode, and $U_{ref,sd}$ is the equilibrium potential for the side reaction.

In the solution phase, lithium ions are governed by a Fick's law of diffusion combined with an intercalation current density term transferring ions between the solution and the solid:

$$\varepsilon_2 \frac{\partial c_2}{\partial t} = \nabla \cdot \left(D_2^{eff} \nabla c_2 \right) + \frac{1 - t^+}{F} J \tag{8}$$

where ε_2 represents the volume fraction of the solution phase, D_2^{eff} denotes the effective diffusion coefficient of lithium in the solution phase, and t^+ stands for the transference number.

The solid phase concentration is governed by a radially symmetric spherical diffusion:

$$\frac{\partial c_{1,j}}{\partial t} = \frac{D_{1,j}}{r^2} \frac{\partial}{\partial r} \left(r^2 \frac{\partial c_{1,j}}{\partial r} \right) \tag{9}$$

where D_1 is the diffusion coefficient of lithium in the solid phase, and r is the sphere radius. This occurs at every point in the anode and the cathode, and is connected to the solution via the intercalation current density.

Finally, a resistive film builds up in the anode as a result of side reaction:

$$\frac{\partial \delta_{film}}{\partial t} = -\frac{J_{sd} M_p}{a_n \rho_p F} \tag{10}$$

with δ_{film} being the thickness of the resistive film, and M_p and ρ_p representing the molecular weight and density of the side reaction product, respectively. This results in resistance increase of the side film:

$$R_{film} = R_{SEI} + \frac{\delta_{film}}{K_p} \tag{11}$$

where R_{SEI} denotes the initial solid electrolyte interface resistance, and K_p represents the conductivity of the side reaction product, respectively.

Equations (1)-(11) form a set of differential algebraic equations (DAEs) that must be solved numerically to simulate the model. There are two major difficulties associated with these DAEs: (*i*) the existence of a very large number of state variables (reasonable discretizations of the equations can yield tens of thousands of state variables), and (*ii*) the presence of a large set of nonlinear algebraic constrains, i.e., Equations (1)-(7), that must be solved at every point along the electrodes in every instant of time.

To resolve the computational issues with the battery model, we use two model reduction methods developed in [26] to simplify the battery model. A quasi-linearization strategy is adopted for linearizing the constraints, and a family of analytic Padé approximations is used to reduce the number of states associated with the spherical diffusion process. These methods enable simulating the model orders of magnitude faster than real-time without compromising accuracy much. The details of these methods are omitted here for brevity but can be found in [26].

B. Battery Model Simulations

In this section, we provide a simulation of the reduced battery model to obtain a useful map that can qualitatively describe the battery degradation behavior. To obtain such a map, we first initialize the battery SOC at different levels through initializing the concentration of lithium ions in the electrodes, and then apply input current signals at different rates to charge and discharge the battery. We monitor the *average* resistance growth rate in the anode at the first step of the simulation, and then plot it as a function of SOC and the input current rate.

Figure 4 depicts the obtained map in a SOC range of 5% to 85% and a charging rate of -2 *C* to 2 *C*, with negative sign indicating discharge. *C*-rate is a standard unit for battery charge and discharge, representing the ratio of the applied current (in Amp) to the rated capacity of battery (in Amp-hour). For instance, at the charge rate of 1 *C* the battery can be fully charged in one hour, whereas at 2 *C* it only takes half hour to charge the battery for a full SOC range.

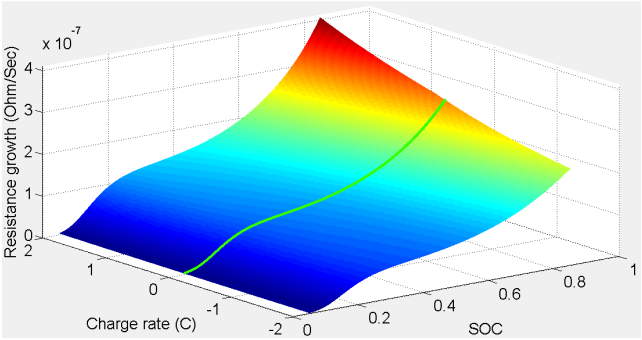

Fig. 4. Battery degradation map.

From Figure 4 we see that at higher SOCs and higher charge rates the battery tends to degrade faster. Particularly, when the applied current is zero (which indicates the battery is at rest,) a substantial degradation can still take place (follow the highlighted line on the surface). Thus, a reasonable strategy for charging Li-ion batteries (based on the degradation model adopted in this paper) is to delay charging toward the time of use such that the battery receives *only the needed charge, right before the time of use*. This way, we can minimize the duration in which battery stays at high SOC; thus we can reduce its degradation. This strategy, namely, delayed charging, will be discussed with more detail in Section 6.

Before moving to the next section, i.e., PHEV charge trajectory optimization, we provide a few important remarks about the battery model:

- In our simulations, *battery voltage* corresponds to the solid phase potential at the rightmost point of the cathode (right collector); *SOC* represents the spatial average of lithium ions concentration in the anode divided by its maximum value; and, the *resistive film growth rate* corresponds to the spatial average of SEI growth rate in the anode.
- For the battery charging simulation, a constant-current constant-voltage (CCCV) strategy is implemented. That is, the charging begins with a constant-current phase, and, if the voltage reaches to the upper limit of 4.2 volts, the applied current decreases in a controlled way to maintain the voltage constant.
- To simulate the system during the discharge phase, first the vehicle model is simulated for the given drive cycle. Then, the electric current signal to the motors is recorded and applied to the electrochemistry-based battery model to obtain the trajectories of SOC, voltage, and resistive film growth during the trip.

It is also important to note that the SOC-dependent degradation trend of the battery model (e.g., higher degradation at higher SOCs) is consistent with the existing empirical trends obtained for Li-ion batteries [7, 8].

In the next section, we will use the PHEV model together with battery model in a multiobjective genetic optimization algorithm to obtain the PHEV optimal charge trajectories.

IV. PHEV Charge Trajectory Optimization

We pursue two objectives for the optimization of PHEV charge trajectory. One objective is to minimize the total energy cost of PHEV for a given daily drive cycle, and the other is to reduce the amount of resistive film growth in the battery anode, and hence improve its useful life. In order to parameterize the charge trajectory for the optimization, we assign variables indicating the "*time*", the "*amount*", and the "*rate*" at which battery receives electricity from the power grid before each trip. The CCCV charging strategy is imposed, unless the battery reaches either to the assigned charge level or to 85% SOC. This particular SOC cap is imposed to avoid excessive damages to the battery due to overcharging.

For a drive cycle with N separate trips the optimization problem is formulated as:

$$\underset{x}{\text{Minimize}}\left\{\begin{array}{l}\left(f_1(x)=\int_{24hr} J_{fuel}(x,t)dt+\int_{24hr} J_{elec}(x,t)dt\right)\\ \&\left(f_2(x)=\bar{R}_{film}^{24hr}(x)\right)\end{array}\right\}$$

$$x=[x_1,x_2,x_3,...,x_{3N}]$$

$$x_{3i-2},\ i=1,2,...,N\ (i.e.\ x_1,x_4,...x_{3N-1})$$

charge start time fore trip i

$$x_{3i-1},\ i=1,2,...,N\ (i.e.\ x_2,x_5,...x_{3N-1})$$

charge rate fore trip i (between 0 and 1C)

$$x_{3i},\ i=1,2,...,N\ (i.e.\ x_3,x_6,...x_{3N})$$

charge amount fore trip i (up to 85% SOC) (12)

where J_{fuel} and J_{elec} are the instantaneous fuel and electricity dollar costs per unit time, $\bar{R}_{film}^{24hr}$ is the final resistance of the anode side film (averaged spatially over the electrode) at the end of the 24-hr simulation, representing the battery degradation, and x is the vector of optimization variables corresponding to the charge trajectory. The upper and lower

bounds of the variables related to the charge time are set to cover the entire time span between the trips.

The explained optimization problem suffers from two conflicting objectives. While minimizing the total energy cost requires high SOC at the beginning of the trips, battery tends to degrade faster at higher SOCs. Therefore, a single optimal point does not exist; instead, an Optimal Pareto front can be obtained. The next section briefly presents a modified genetic algorithm developed for multiobjective optimization problems, which will be applied in this paper to obtain optimal PHEV charge trajectories.

V. Non-dominated Sorting Genetic Algorithm

Several modified genetic algorithms have been developed for multiobjective optimization problems. Niche genetic algorithm [27, 28] and non-dominated sorting genetic algorithm II (NSGA-II) [16] are among the most widely used methods. Particularly, NSGA-II has several advantages in terms of computational efficiency and elitism, which makes it a suitable choice for our optimization problem here.

NSGA-II follows the fundamentals of basic genetic algorithm with a difference in the selection criterion. In this algorithm, the fittest solutions are selected based on their non-domination ranking and crowding distance. The non-domination ranking of an individual is determined by comparing it to the other individuals in the same generation and counting the number of individuals that dominate it along all objectives. Figure 5 demonstrates an initial population distribution in a double-objective optimization problem. If we consider minimizing both objectives, the non-domination ranking of a solution can be determined by counting the number of solutions entrapped in its lower left area (or the domination zone). For example, the solutions with non-domination rank of 1 have no other solutions in their domination zone. Similarly, a solution with the non-domination rank of 6 has 5 solutions entrapped in its domination zone. Solutions belonging to the same non-domination rank divide the population into multiply layers of equally-ranked members.

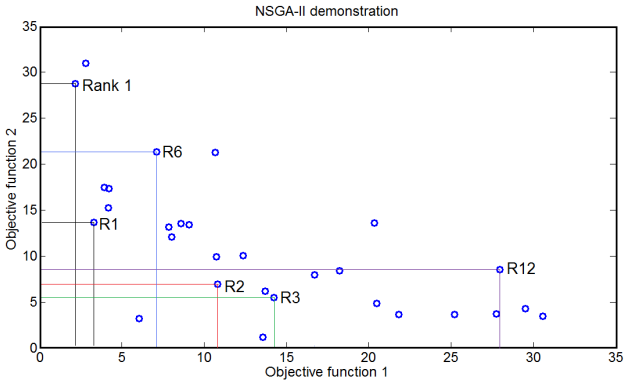

Fig. 5. Determining the non-domination rank of solutions in a population.

In every generation of NSGA-II, only half of the parents/children population can proceed to the next generation. Once the fronts are sorted according to their non-domination rank, those with better rank proceed to the next level. There might, however, be a marginal front whose members exceed the number of remaining open slots. In that case, another criterion, namely, the crowding distance, is used to select the succeeding solutions. The crowding distance measures the average distance of a solution from its neighboring solutions along each of the objectives. In a marginal front, the solutions with larger crowding distance are ranked better. This leads to obtaining a more uniform distribution of the Pareto front. Once the selection process is over, usual binary tournament selection, recombination and mutation operators are used to create the next generation. Interested readers are encouraged to study [16] for more details of NSGA-II.

VI. PHEV Charge Trajectory Optimization

Having set up all the necessary tools for PHEV simulation and optimization, we can implement NSGA-II to obtain the PHEV optimal charge trajectories. According to the optimization formulation, Eq. (12), three optimization variables are dedicated for each active segment of a given drive cycle. The simulations in this section are based on the 24-Hr naturalistic drive cycle with two half trips shown in Figure 2, resulting in six optimization variables.

To calculate the amount of electric energy price for every charging schedule, the pricing policy of the DTE Energy Company is used [19]. For the electric vehicles, this policy breaks into two periods over a year and two on-peak and off-peak segments. For the period of June to September and during the on-peak hours (10.00 am until 7.00 pm) the electricity rate is 0.099 USD/kWh, while during the off-peak hours this rate reduces to 0.035 USD/kWh. The on-peak electricity rate changes to 0.047 USD/kWh during the period of October through May. In this study, we choose the pricing policy of June to September.

The optimization result is shown in Figure 6, where after 60 generations of 80 populations, a Pareto front is formed from the initial distribution of the PHEV charge trajectories. The total energy cost ranges between $1.6 and $2.7 for the solutions belonging to the Pareto front. On the other hand, the amount of added battery resistance varies from 7.9 to 13.5 milliohms. Hence, a wide range of feasible solutions exist for this problem. We choose three critical points from the Pareto front (marked by numbers in Figure 6) and plot their corresponding charge trajectories in Figure 7 for a qualitative comparison. We also plot the drive cycle and the electricity pricing profile in Figure 7.

The first choice (marked by #1 in Figure 6) corresponds to the solution with the least battery degradation. There is no charge added to the battery, and SOC remains at the lowest level for the entire day. This is essential to keep the battery degradation minimal based on the discussion provided in Section III. Hence, the charge trajectory of the PHEV remains at zero for the entire day.

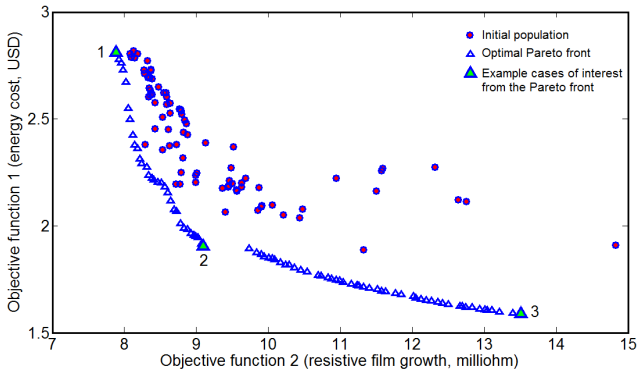

Fig. 6. Pareto front type solution for the optimal charge trajectory of PHEV obtained through NSGA-II.

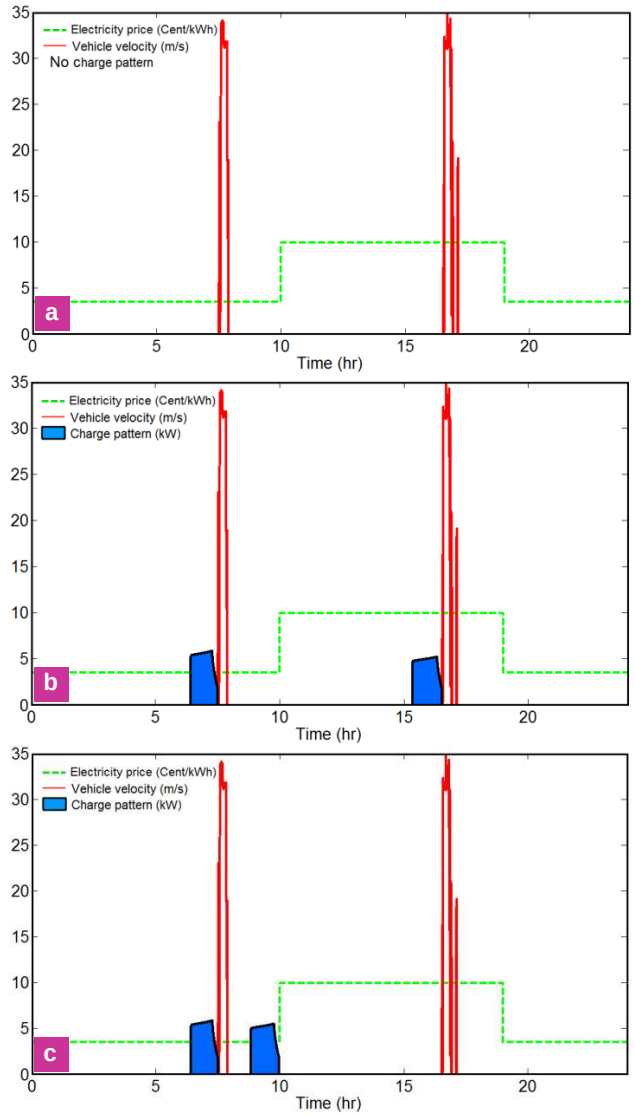

Fig. 7. Optimal charge trajectories for PHEVs: (a) for the best battery health, (b) for a balanced tradeoff between battery health and energy cost, and (c) for the least energy cost.

The second choice (marked by #2 in Figure 6) represents a balanced tradeoff between the battery health and the energy cost objectives. Figure 7(b) depicts the charge trajectory for this scenario. Charging starts before each trip at a high rate in such a way that the battery reaches its maximum SOC limit just before the trip starts. On the one hand, the battery has a high SOC at the beginning of the trips, thus the overall energy cost remains low at the end of the day. On the other hand, the PHEV depletes the battery charge immediately after the charging is finished. Thus, the high-rate resistive film growth takes place only for a short period of time.

The last case of interest (the point marked by #3 in Figure 6) corresponds to the charge trajectory with the least energy cost. In this solution, not only the battery receives sufficient charge before the trips, but also charging takes place during the off-peak hours, where the electricity price is low. The resulting charge trajectory is shown in Figure 7(c). Since the optimality of battery health is also taken into account, the second charging task is delayed until before the jump of electricity price.

The charge trajectories shown in Figure 7(b) and 7(c) demonstrate a slow increase in the charge rate followed by a rapid drop towards the end of charging. This specific charge profile is due to the fact that during the constant-current phase of charging, the battery SOC adds up, increasing the open circuit potential of battery. Therefore, the instantaneous battery power demand increases accordingly. When the battery potential reaches its upper limit, the charging strategy turns to the constant-voltage phase, where the applied current drops in a controlled way to maintain the voltage constant. This results in the rapid drop of battery power demand at the end of charging.

Although the results presented in this paper reveal some of the key features of PHEV optimal charge trajectories, further investigations are required to generalize the obtained results. In this respect, the future work of this study will include optimizing and analyzing the PHEV charge trajectory for different battery sizes, vehicle models, drive cycles, and pricing policies. Moreover, the developed methodology will be used for the prediction of aggregate PHEV power demand.

VII. Conclusion

This paper investigates the problem of optimizing PHEV charge trajectory for simultaneous reduction of energy cost and battery degradation. A PHEV model, a battery degradation model, and a multiobjective genetic algorithm were used to optimize the PHEV charge trajectory for a 24-hour naturalistic drive cycle. The optimization results in the formation of a Pareto front on which the objectives are traded off optimally. The comparison of different solutions from the Pareto front indicates that to effectively minimize battery degradation and energy costs, a delayed charging strategy must be used. We expect that the obtained optimal charging strategies will improve the long-term economic benefits of PHEVs, and enhance the prediction of PHEV-related electric load on the power grid.

REFERENCES

[1] Kempton W., Tomic J., 2005. Vehicle-to-grid power fundamentals: calculating capacity and net revenue. Journal of Power Sources, 144, 268-279.

[2] Kempton W., Tomic J., 2005. Vehicle-to-grid power implementation: From stabilizing the grid to supporting large-scale renewable energy. Journal of Power Sources, 144, 280-294.

[3] Marano V., Rizzoni G., 2008. Electric and economic evaluation of PHEVs and their interaction with renewable energy sources and the power grid. Proceedings of the 2008 IEEE International Conference on Vehicular Electronics and Safety, Columbus, OH.

[4] Guille C., Gross G., 2009. A conceptual framework for the vehicle-to-grid (V2G) implementation. Energy Policy, In Press.

[5] Hadley S., Tsvetkova A., 2008. Potential impacts of Plug-in Hybrid Electric Vehicles on regional power generation. ORNL/TM report.

[6] Markel T., Pesaran A., 2007. PHEV energy storage and drive cycle impacts. 7th Advanced Automotive Battery Conference, Long Beach, CA.

[7] Ichimura M., Shimomura M., Takeno K., Shirota R., Yakami J., 2005. Synergistic effect of charge/discharge cycle and storage in degradation of lithium-ion batteries for mobile phones. 27th International Conference on Telecommunications, 245-250.

[8] Jungst R. G., Nagasubramanian G., Case H. L., Liaw B. Y., Urbina A., Paez T. L., Doughty D. H., 2003. Accelerated calendar and pulse life analysis of lithium-ion cells. Journal of Power Sources, 119, 870-873.

[9] Peterson S. B., Apt J., Whitacre J. F., 2009. Lithium-ion battery cell degradation resulting from realistic vehicle, and vehicle-to-grid utilization. Journal of Power Sources (available online).

[10] Kim Y. H., Ha H. D., 1997. Design of interface circuits with electrical battery models. IEEE Transactions on Industrial Electronics, 44, 81-86.

[11] Moss P. L., Au G., Plichta E. J., Zheng J. P., 2008. An electrical circuit for modeling the dynamic response of Li-ion polymer batteries. Journal of the Electrochemical Society, 155, A986-A994.

[12] Doyle M., Fuller T. F., Newman J., 1993. Modeling of galvanostatic charge and discharge of Lithium/polymer/insertion cell. Journal of Electrochemical Society, 140, 1526-1533.

[13] Fuller T. F., Doyle M., Newman J., 1994. Simulation and optimization of the dual Lithium ion insertion cell. Journal of Electrochemical Society, 141, 1-10.

[14] Ramadass P., Haran B., Gomadam P., White R., Popov B., 2004. Development of first principles capacity fade model for Li-ion cells. Journal of Electrochemical Society, 151, 196-203.

[15] Arora P., White R., 1998. Capacity fade mechanisms and side reactions in lithium-ion batteries. Journal of Electrochemical Society, 145, 3647-3667.

[16] Deb K., Pratap A., Agarwal S., Meyarivan T., 2002. A fast and elitist multiobjective genetic algorithm: NSGA-II. IEEE Transactions on Evolutionary Computation, 40, 181-197.

[17] Moura S. J., Fathy H. K., Callaway D. S., Stein J. L., 2008. A stochastic optimal control approach for power management in plug-in hybrid electric vehicles. Proceedings of the 2008 ASME Dynamic Systems and Control Conference, Ann Arbor, MI.

[18] Moura S. J., Callaway D. S., Fathy H. K., Stein J. L., 2010. Tradeoffs between battery energy capacity and stochastic optimal power management in plug-in hybrid electric vehicles. To appear in the Journal of Power Sources.

[19] DTE Energy website, Residential Electric Rates: (http://www.dteenergy.com/residentialCustomers/billingPayment/rates/electric/resRates.html)

[20] O'Keefe M. P., Markel T., 2006. Dynamic programming applied to investigate energy management strategies for a plug-in HEV. National Renewable Energy Laboratory, Golden, CO, Report # NREL/CP-540-40376.

[21] Gong Q., Li Y., Peng Z. R., 2008. Trip-based optimal power management of plug-in hybrid electric vehicles. IEEE Transactions on Control Systems Technology, 57, 3393-3401.

[22] Plett G. L., 2004. Extended Kalman filtering for battery management systems of LiPB-based HEV battery packs: Part 1. Background. Journal of Power sources, 134, 252-261.

[23] Plett G. L., 2004. Extended Kalman filtering for battery management systems of LiPB-based HEV battery packs: Part 2. Modeling and identification. Journal of Power sources, 134, 262-276.

[24] Plett G. L., 2004. Extended Kalman filtering for battery management systems of LiPB-based HEV battery packs: Part 3. State and parameter estimation. Journal of Power sources, 134, 277-292.

[25] Verbrugge M., 2007. Adaptive, multi-parameter battery state estimator with optimized time-weighting factors. Journal of Applied Electrochemistry, 37, 605-616.

[26] Forman J., Bashash S., Fathy H. K., Stein J. L., 2010. Model reduction of a degrading electrochemical Li-ion battery model via constraint linearization and Padé approximation. Submitted to the Journal of Electrochemical Society.

[27] Fonseca C. M., Fleming P. J., 1993. Genetic algorithm for multi-objective optimization: Formulation, discussion, and generalization. Proceedings of Fifth International Conference on Genetic Algorithms, San Mateo, CA.

[28] Horn J., Nafploitis N., Goldberg D. E., 1994. A niched Pareto genetic algorithm for multiobjective optimization. Proceedings of the first IEEE Conference on Evolutionary Algorithms, NJ: IEEE Press.